ornl

OAK
RIDGE
NATIONAL
LABORATORY

UNION
CARBIDE

OPERATED BY
UNION CARBIDE CORPORATION
FOR THE UNITED STATES
DEPARTMENT OF ENERGY

NUREG/CR-2661
ORNL/TM-8295

Flaw Measurement Using Ultrasonics In Thick Pressure Vessel Steel

K. V. Cook
P. J. Latimer
R. W. McClung

Prepared for the U.S. Nuclear Regulatory Commission
Office of Nuclear Regulatory Research
Under Interagency Agreement DOE 40-551-75

Printed in the United States of America. Available from
National Technical Information Service
U.S. Department of Commerce
5285 Port Royal Road, Springfield, Virginia 22161

Available from

GPO Sales Program
Division of Technical Information and Document Control
U.S. Nuclear Regulatory Commission
Washington, D.C. 20555

NUREG/CR-2661
ORNL/TM-8295
Distribution
Category R5

Contract No. W-7405-eng-26

METALS AND CERAMICS DIVISION

FLAW MEASUREMENT USING ULTRASONICS IN THICK PRESSURE VESSEL STEEL

K. V. Cook, P. J. Latimer, and R. W. McClung

Manuscript Completed — June 1982

Date Published — August 1982

Prepared for the
U.S. Nuclear Regulatory Commission
Office of Nuclear Regulatory Research
Washington, DC 20555
Under Interagency Agreement DOE 40-551-75
NRC FIN No. B0103

Prepared by
OAK RIDGE NATIONAL LABORATORY
Oak Ridge, Tennessee 37830
operated by
UNION CARBIDE CORPORATION
for the
DEPARTMENT OF ENERGY

CONTENTS

ABSTRACT 1
INTRODUCTION 1
DESCRIPTION OF EQUIPMENT AND MATERIALS 2
ELECTRONIC 2
SEARCH UNITS 2
MATERIALS AND MECHANICAL APPARATUS 2
PROCEDURES USED 9
LENGTH MEASUREMENTS 9
DEPTH MEASUREMENTS 9
RESULTS AND DISCUSSION 11
SURFACE FLAWS 11
Length Measurements 13
Correlation Between the Magnitude of Lateral Beam Spread and Flaw Length Measurements 16
Beam Spread Corrections for Length Measurements . . . 17
Depth Measurements 19
BURIED FLAWS 22
CONCLUSIONS AND RECOMMENDATIONS 23
ACKNOWLEDGMENTS 24
REFERENCES 24
Appendix. THE INFLUENCE OF THE ANGULAR ORIENTATION OF THE SEARCH UNIT UPON THE RECEIVED AMPLITUDE FROM THE FLAW 25

FLAW MEASUREMENT USING ULTRASONICS IN THICK PRESSURE VESSEL STEEL

K. V. Cook, P. J. Latimer,* and R. W. McClung

ABSTRACT

The net effects of such variables as beam width, beam angle, and flaw geometry were considered with regard to their total impact upon flaw measurement. The boundaries of accuracy and repeatability were established for the manual measurement of a limited number of flaws by the American Society of Mechanical Engineers code procedures. Both surface and buried reflectors were considered, and changes were recommended in both the detection and measurement of buried midplane flaws. Correlations were made between the magnitude of lateral beam spread and length measurements. Approximate corrections for lateral beam spread were applied to measurements of large flaw lengths. Correlations were made between code-measured flaw depths and real depths on a limited number of flaws of various depths and orientations. Finally a brief study was made to determine the influence of the angular orientation of the search unit upon the received amplitude from the flaw.

INTRODUCTION

In the American Society of Mechanical Engineers *ASME Boiler and Pressure Vessel Code* (code), Article 4 of Sect. V on Nondestructive Examination deals with ultrasonic examination for measurement of indications. It is essential that the net effects of variables such as beam width, beam angle, and flaw geometry be considered with regard to their total impact upon flaw measurement.

The primary purpose of the confirmatory work reported here was to establish the boundaries of accuracy and repeatability in manual measurement of flaws by the code procedure. The flaws considered in this work include surface and buried flaws. One set of surface flaws consisted of a series of circular-saw notches oriented at various angles relative to the surface. The other set of surface flaws consisted of machined notches and electron beam (EB) weld cracks produced by the hydrogen embrittlement process.[1] A midplane or buried simulated flaw was also used. This simulated flaw was made with vertical saw cuts tangential to a midplane side-drilled hole (fabrication details will be provided later).

Secondary topics considered in this work include the development of a supplementary technique for the measurement of flaw depths in those cases where the half-maximum amplitude indication from the flaw exceeded 100%

---

*University of Tennessee, Knoxville.

full-screen height. It was necessary to extrapolate that supplementary technique because the code omitted any specific reference to flaw indications in that category.

The influence of lateral beam width in the determination of flaw length was briefly considered. The beam width corrections reported here are very preliminary and approximate, but they represent the first step toward a more sophisticated approach. We noted that any slight changes in the angular orientation of the search unit made significant changes in the manual measurement of flaw lengths and depths. A brief study was made to determine the effects of search unit orientation upon received amplitude. The results of that study are presented in the appendix.

The results reported here are restricted to the conditions most commonly used with code procedures: 2.25-MHz, 25.4-mm-diam (1.00-in.) circular transducers on plastic wedges that produce shear waves with beam angles of 45 and 60°.

DESCRIPTION OF EQUIPMENT AND MATERIALS

ELECTRONIC

Two commercial instruments typical of those used in field applications were employed in these studies. Most of the data were collected with an instrument arbitrarily referred to as instrument II. This instrument was operated with the receiver tuning switch in the 2-MHz position, where the bandwidth at −20 dB extends from 1.5 to 5.9 MHz with a center frequency of 2.8 MHz.[2] The limited use of instrument I for these studies is reported in the section on Correlation Between Magnitude of Lateral Beam Spread and Flaw Length Measurements. The instrument I characteristics, as used, are also addressed in that section. Before data collection, both instruments were calibrated and checked in accordance with the requirements of the ASME code.

SEARCH UNITS

The commercial transducer used for the work reported here was a 2.25-MHz untuned unit. It was circular with a diameter of 25.4 mm (1.00 in.). The ORNL serial number for the transducer was U-3. The transducer was used in conjunction with 45 and 60° commercially manufactured plastic wedges listed by ORNL serial numbers NRC 2 in each case.

MATERIALS AND MECHANICAL APPARATUS

All the specimen blocks used in this study were constructed from unclad pressure vessel steel. A calibration block patterned after the ASME code (Figs. 1 and 2) was constructed from a steel plate purchased from Combustion Engineering, Inc., (CE) of Chattanooga, Tennessee. The CE material was SA-533 grade B class 1 steel plate and was given, in addition to normal quench and temper, a stress-relief heat treatment to simulate

ORNL-PHOTO 3249-77

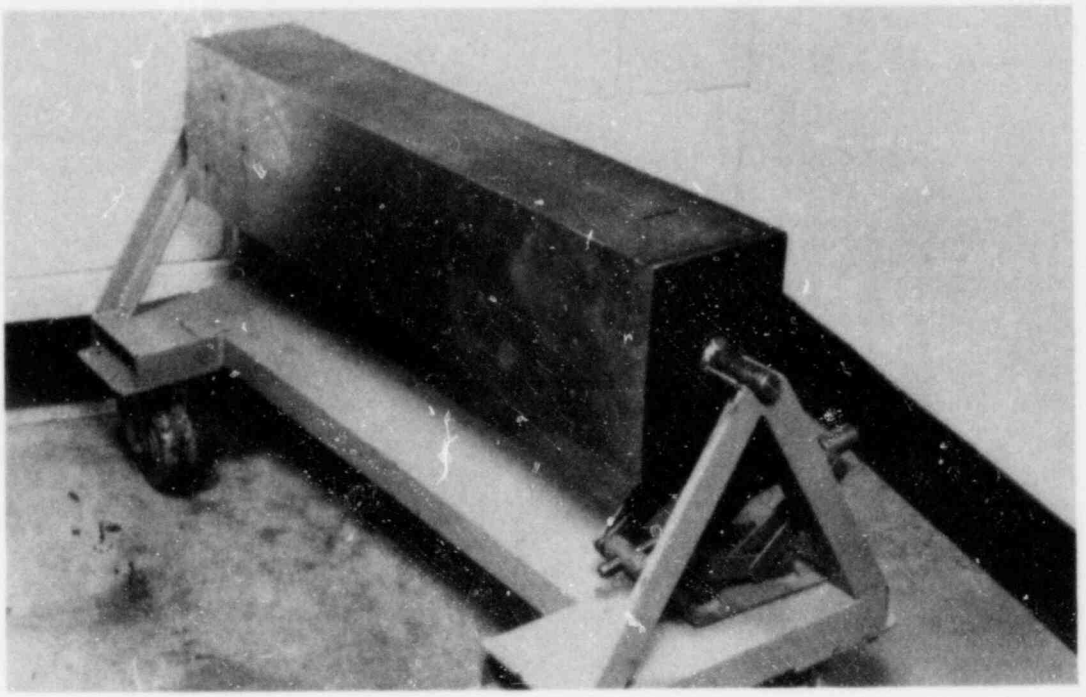

Fig. 1. The calibration block patterned after ASME code.

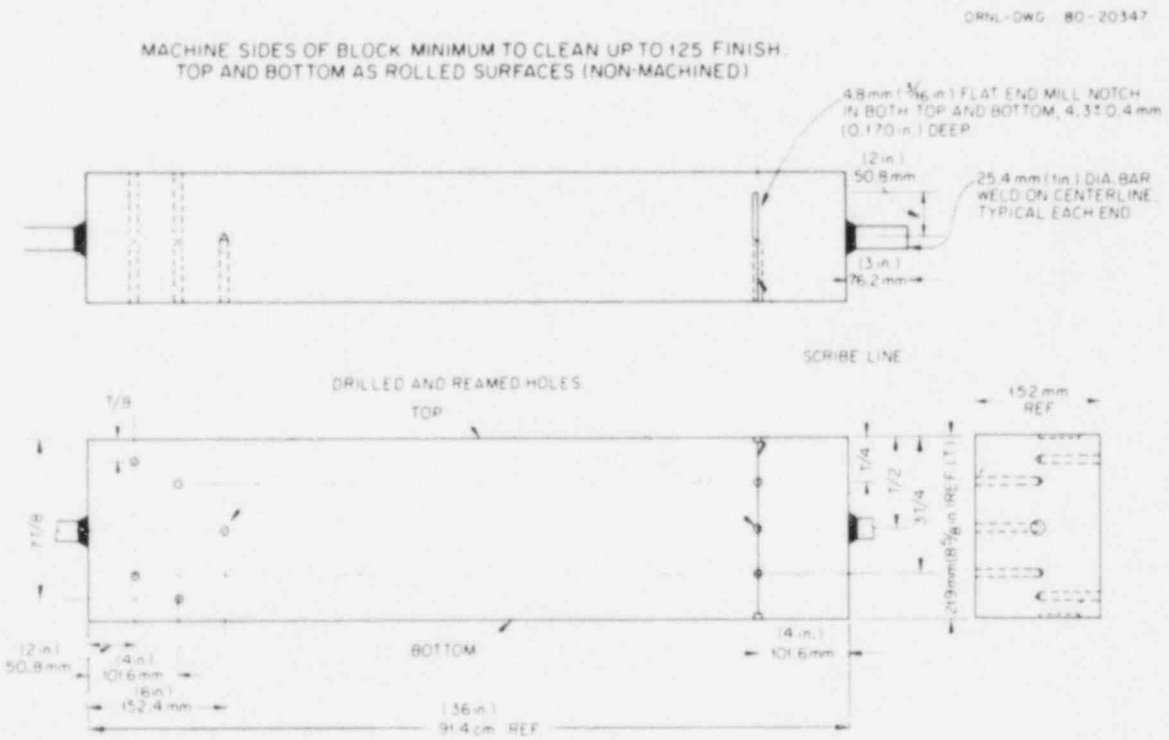

Fig. 2. Diagram of calibration block patterned after ASME code.

postweld heat treatment imposed on a reactor vessel. Side-drilled holes with a diameter of 9.5 mm (0.375 in.) were drilled into the blocks to conform to the ASME code requirements of Article 4, Sect. V.

Specimen block 3 was used for the introduction of artificial circular flaws. It was constructed from a plate provided by Lukens Steel Company. The material was grade B (Lukens heat B-1258-2) steel plate edge trimming. The block was machined to dimensions of 940 by 254 by 178 mm (37.0 by 10.0 by 7.5 in.) and a surface finish of RMS 125. The notches were introduced by an abrasive circular saw with a blade diameter of 101.6 mm (4.00 in.). The saw was mounted on a milling machine attachment from a lathe. The combination was used with a magnetic chuck and dial gage indicator to cut notches with a controlled depth and angle (see Fig. 3).

Ten notches were cut into the surface of block 3. Each notch had a circular cross section with a 0.43-mm (0.017-in.) width by about 41-mm (1.6-in.) length by a maximum depth of 4.6 mm (0.18 in.) (see Fig. 4). Six notches were introduced in two rows of three with 76 mm (3.0 in.) separating the adjacent notches. The notches had angles of entry of +15, +30, +45, −15, −30, and −45° respective to the normal of the primary inspection surface. Another notch (notch 4) was introduced at 0° (perpendicular to the primary inspection surface) (see Figs. 4 and 5). Rubber replicas were made and used to check on the sizes and angles of the notches (Fig. 6).

ORNL-PHOTO 3251-77

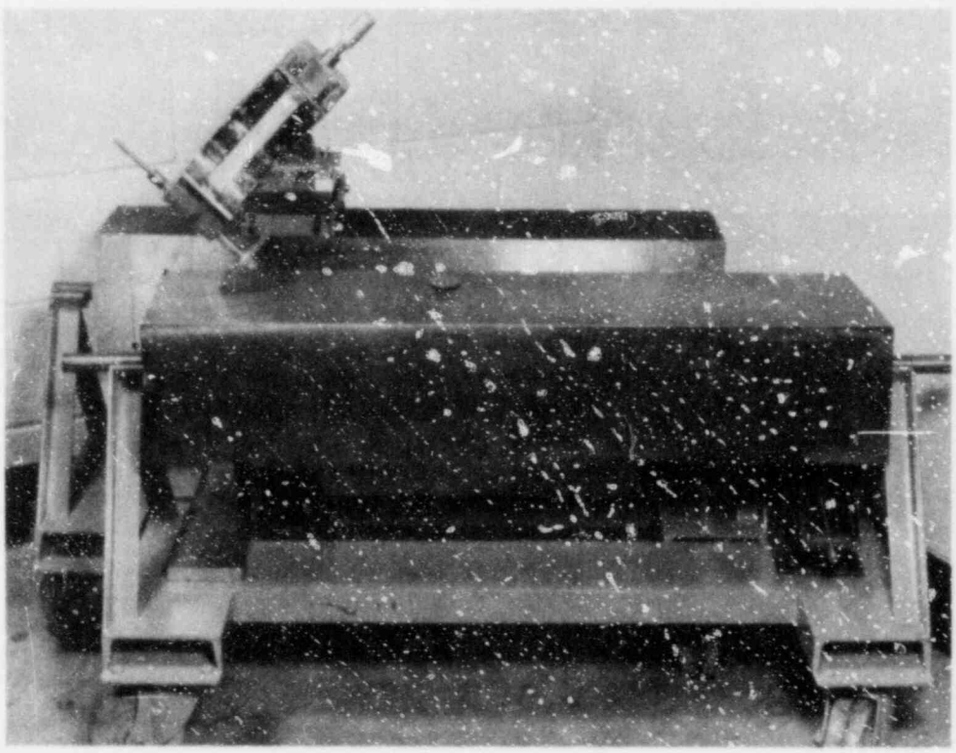

Fig. 3. Abrasive saw used for cutting angled circular notches (block 3).

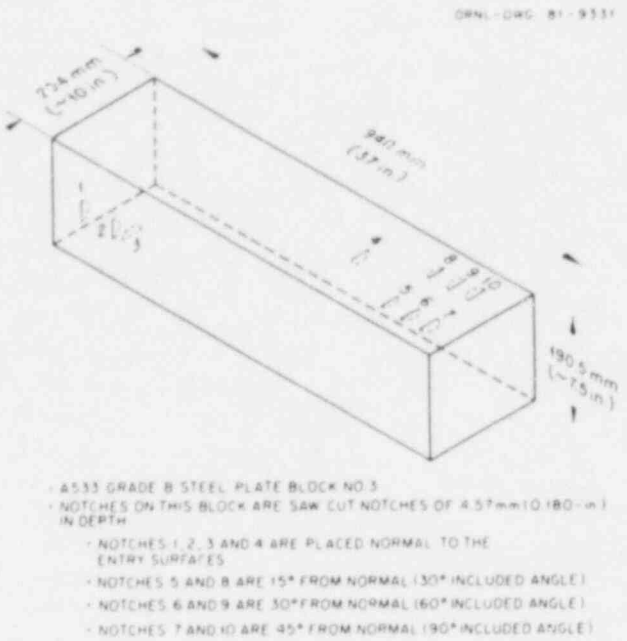

Fig. 4. Specimen block 3, showing positions of notches.

ORNL-PHOTO 0879-78

Fig. 5. Surface of block 3.

ORNL-PHOTO 0876-78

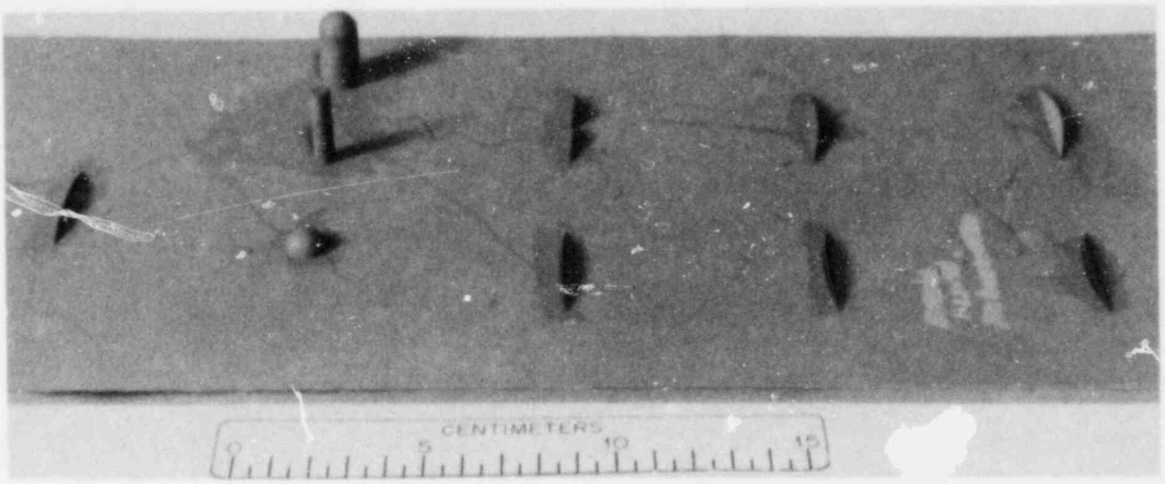

Fig. 6. Rubber replicas for flaws in specimen block 3.

Specimen block 2 was prepared with a buried flaw. It was introduced into the block by first making a side-drilled hole [15.9 mm (5/8 in.)] at a depth of one-half the thickness of the block (Fig. 7). From the SDH, vertical cuts were placed tangential to the hole. When examined ultrasonically with an angle beam, the tangential saw cuts approximated a midplane flaw in the specimen block. The saw cut was 38 mm (1.5 in.) deep (Fig. 8). Surface flaws were also introduced into block 2 so that they duplicated those in block 4. These surface flaws are described in the following paragraph.

Specimen block 4 was constructed from type A 533 grade B Lukens heat B-1258-2 steel and machined to dimensions of 1209 by 228 by 177.8 mm (47 5/8 by 9.0 by 7.00 in.). A number of surface flaws were introduced into the block in the form of electrodischarge-machined (EDM) notches, electron beam (EB) weld cracks, and a saw cut. The EB welds were cracked by the hydrogen embrittlement[1] process to more closely simulate a natural crack. Figure 9 shows a typical cross section of an EB weld crack produced in A 533 steel plate. The geometry of the EDM notches is illustrated in Fig. 10. The EDM slots simulated rectangular flaws [about 80 mm long (3 in.)] with rounded corners (flaws 1 and 2). The plane of the EDM slots was oriented perpendicular to the surface, and they had a depth of either 12.7 or 6.35 mm (0.50 or 0.250 in.). The EB weld cracks (flaws 3 and 6) each had lengths about 80 mm (3 in.) and depths of 9.5 mm (3/8 in.). The plane of the cracks was oriented perpendicular to the surface of the block. The saw cut (flaw 5) had a surface length of 48 mm (1.9 in.) and a depth of 5.6 mm (0.22 in.). Again the circular cross-section cut was oriented in a plane perpendicular to the block surface.

ORNL-PHOTO 0878-78

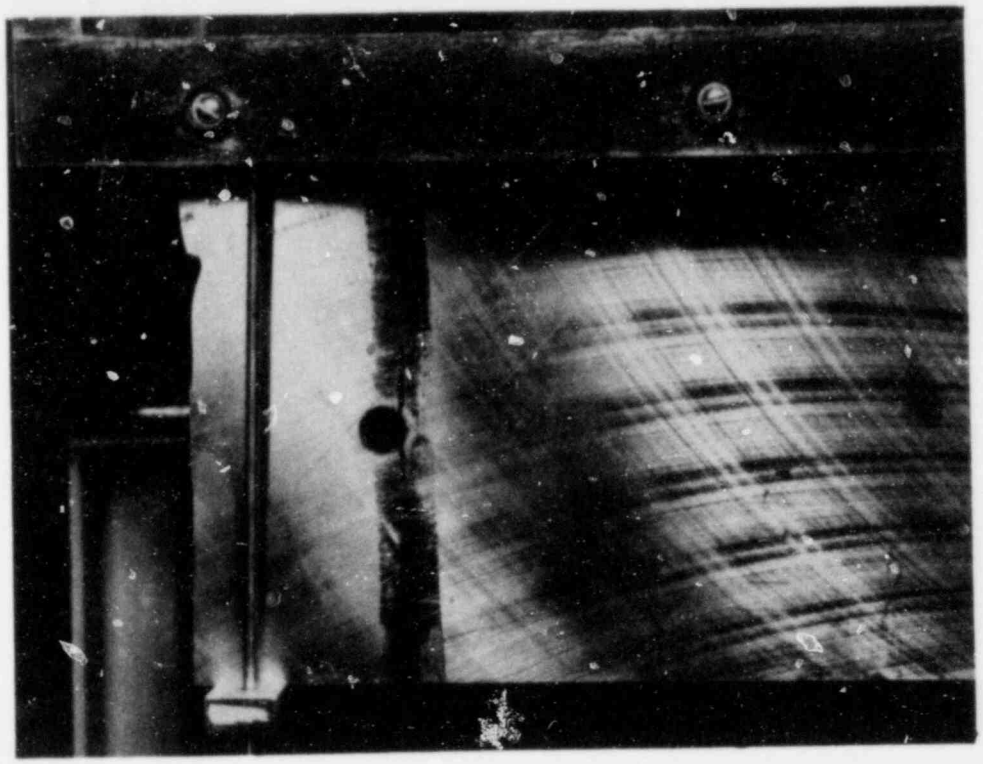

Fig. 7. The specimen block that contains a buried simulated flaw.

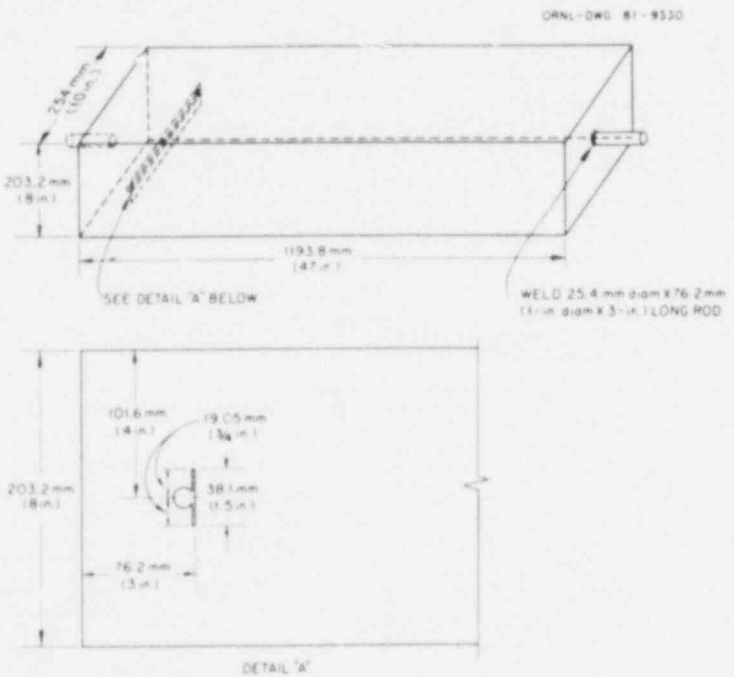

Fig. 8. The specimen block with a midplane or buried simulated flaw.

Y-158205

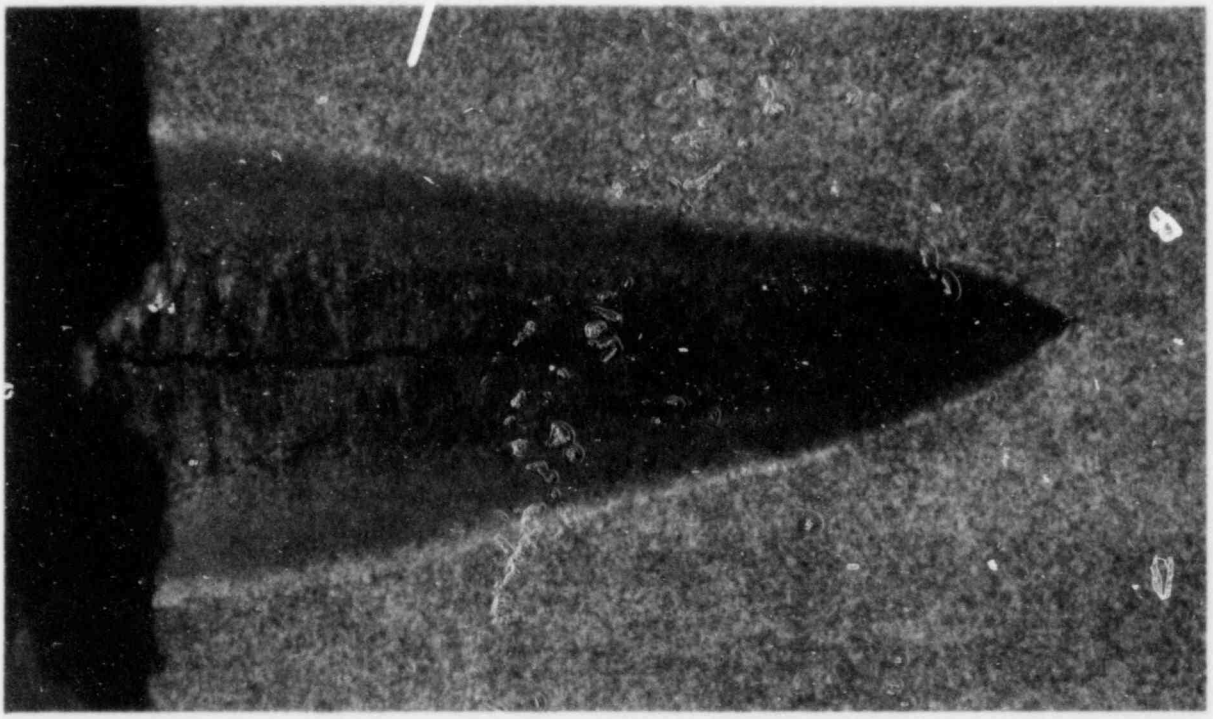

Fig. 9. Cracked electron-beam weld in a piece of A 533 steel plate. The crack was produced by a hydrogen charging technique.

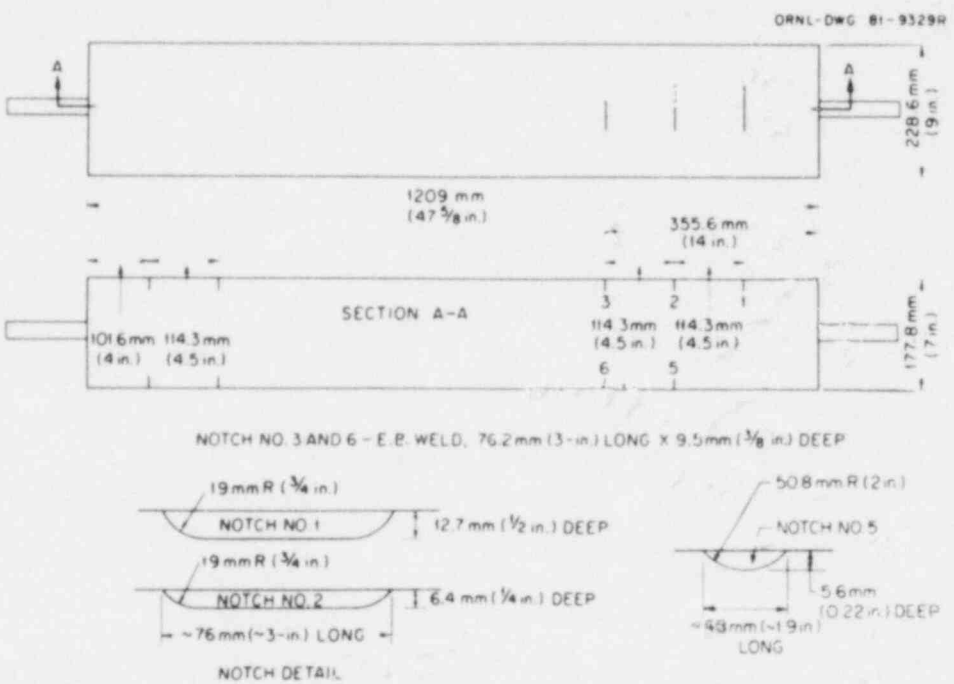

Fig. 10. Specimen block containing the electrodischarge-machined notches and EB weld cracks (block 4).

PROCEDURES USED

All measurements for this work were made with a water box (shallow water coupling). Before taking data, we checked the screen height linearity and amplitude control linearity according to the procedures given in Mandatory Appendices I and II to Article 4 of the code. Sweep range calibration and distance amplitude corrections (DACs) were made in accordance with Nonmandatory Appendix B to Article 4. The DAC curve was drawn on graph paper for a permanent record, and also the 100% and 50% DAC curves were drawn directly on the instrument screen with a grease pencil.

In all instances the scanning in this study (except in the appendix) was done manually. The maximum amplitude from each flaw indication in percent DAC and the corresponding sweep position were recorded as the initial step in data acquisition. All flaw length and depth measurements were made with the flaw on the opposite surface from the search unit (V/2 shear-wave path).

LENGTH MEASUREMENTS

The length of the flaw in each case was measured strictly by code procedures: the distance between the positions of the search unit at the 50% DAC points on the ends of the reflector was recorded as the length of the reflector. The primary purpose of this confirmatory work was to set the boundaries on accuracy and repeatability of measurements of flaw dimensions by manual scanning. Therefore, instead of repeating each measurement of length three times as suggested by the Code, we repeated each at least ten times. In most instances one-half the data were collected by one operator and the other half collected independently by another operator to minimize bias introduced into the results by the judgment of the operator. The mean and standard deviation were then determined for each data set corresponding to a particular flaw. The means were compared with the actual known flaw lengths, and the calculated percentage errors were used as an indication of the accuracy of the method. The standard deviations were used to indicate the overall abililty to repeat the measurements (i.e., the standard deviation was expressed as a percentage of the actual flaw length or depth). In addition, the data from each independent operator were cross-checked for general agreement.

DEPTH MEASUREMENTS

Depths were measured according to percentage DAC indications as prescribed by Appendix D-10, Article 4, Sect. V, of the code in those instances where the amplitude of the signal did not exceed the limits of linearity of the screen. The following is a discussion of the various conditions observed in this study for measuring flaw depth.

1. For reflectors 50 to 100% DAC, minimum sweep readings were read from the flaw detector's display at 50% DAC when the reflector was

approached from the minimum signal direction. Maximum sweep readings were also read from the flaw detector screen at 50% DAC when moving away from the reflector's maximum signal direction.

2. For reflectors exceeding 100% DAC, the 50% maximum amplitude (taking into account DACs) curve was drawn on the screen. Minimum sweep readings were taken at 50% maximum amplitude when approaching the reflectors from the maximum signal direction. Maximum sweep readings were taken when moving away from the reflector's maximum signal direction.

In both instances the difference between the maximum and minimum calibrated sweep readings was then used to calculate the depth in length units and in percent t (where t represents the block thickness).

3. In many cases, particularly when using a 45° beam, we found that not only was the signal from the reflector deflected off screen, but in addition the half-maximum amplitude exceeded 100% full screen height (FSH). This situation is not specifically covered by code procedures. As a result, we needed to develop a supplementary procedure to determine depth for indications of that type.

The following is a brief description of the various procedures that were used:

1. Reduce maximum signal amplitude to 80% FSH and take sweep readings at half-maximum amplitude (taking DAC into account) approaching and receding from the maximum amplitude direction.

2. Reduce maximum signal amplitude to 100% DAC and take sweep readings at 50% DAC approaching and receding from the maximum signal.

3. Reduce maximum signal amplitude to 80% FSH and take sweep readings at 50% DAC approaching and receding from the maximum signal.

4. Reduce maximum signal amplitude to 80% FSH and take sweep readings at 100% DAC approaching and receding from the maximum signal.

5. Reduce signal amplitude to 80% FSH and take sweep readings at 40% FSH approaching and receding from the maximum signal (no DAC).

6. Reduce the maximum amplitude in steps of 6 dB until the reduced signal amplitude does not exceed 100% FSH and then take sweep readings at half-maximum amplitude approaching and receding from the maximum amplitude.

7. Leave the signal amplitude deflected off screen and take sweep readings at 50% DAC approaching and receding from the maximum amplitude.

Of the procedures that were evaluated, the method that we selected was the one described as item 1 above. This procedure was adopted because it was simple and closely resembled the code procedure for reflectors exceeding 100% DAC. *Furthermore, this technique was adopted for all cases where the maximum amplitude was deflected off screen* (i.e., more than 100% FSH).

As in the case of length data, the depth data were taken in data sets with a minimum of ten independent readings. Also, in most instances two different operators took half of each data set for the reasons previously discussed. The mean for each data set was compared with the known depth of the flaw to arrive at an indication of the accuracy of the measurement, and the standard deviation was used as an indication of the ability to repeat the measurement.

RESULTS AND DISCUSSION

SURFACE FLAWS

A description of each surface flaw considered in this work appears in Tables 1 and 2. Also included in Tables 1 and 2 is the maximum amplitude indication from each flaw expressed as a percentage DAC (established on the calibration block shown in Fig. 1) for both 45 and 60° beam angles. The maximum amplitude in percent DAC was read directly from the flaw detector screen (i.e., as described by the Code) or calculated as shown in the example in Table 2 when FSH was exceeded.

Table 1. Description of flaws[a] in block 3 (see Fig. 4) (saw-cut notches at different angles)

Flaw	Notch depth,[b] (mm)	Notch depth,[b] (in.)	Angle of orientation,[c] θ	Maximum amplitude (% DAC)[d] for each beam angle, 45°	Maximum amplitude (% DAC)[d] for each beam angle, 60°
4	4.6	0.18	0° normal to surface	800	200
5	4.4	0.17	15° away from search unit	150	100
8	4.4	0.17	15° toward search unit	150	200
6	4.0	0.16	30° away from search unit	150	600
9	4.0	0.16	30° toward search unit	250	550
7	3.2	0.13	45° away from search unit	500	*e*
10	3.2	0.13	45° toward search unit	250	150

[a]Most notches are marginally unacceptable by Table IWB-3510.1 of Sect. XI of the ASME code.

[b]All notches are about 41 mm long on the surface and of elliptical shape (see Figs. 4–6). The depths of the angled notches were calculated from the relation of d (mm) = 4.6 cos θ.

[c]Measured relative to the surface normal.

[d]Maximum amplitude in % DAC = flaw amplitude relative to 100% DAC.

[e]Not measurable with 60° beam.

Table 2. Description of flaws[a] in block 4 (see Fig. 10) (machined notches and electron-beam weld cracks)

Flaw	Description	Dimensions, mm (in.)		Maximum amplitude (% DAC)[b] for each beam angle	
		Length	Depth	45°	60°
1	Machined notch	74.7 (2.94)	12.7 (0.5)	1650	950
2	Machined notch	69.9 (2.75)	6.4 (0.25)	950	500
3	EB weld crack	76.2 (3.0)	9.5 (0.375)	900	500
5	Saw-cut	48.0 (1.9)	5.6 (0.22)	850	400
6	EB weld crack	76.2 (3.0)	9.5 (0.375)	850	400

[a]All discontinuities unacceptable by Table IWB-3510.1 of Sect. XI of the ASME code.

[b]Maximum amplitude in % DAC = relative flaw amplitude to 100% distance amplitude correction.

Example 1: Read directly from flaw detector screen and superimposed DAC curve.

Example 2: Calculate if flaw signal exceeds full screen height using the following:

1. Attenuate the maximum flaw signal with the calibrated attenuator on the flaw detector to change the saturated signal to about 100% DAC.
2. Estimate from the flaw detector screen and superimposed DAC curve the amplitude of the attenuated signal (A_1) as a percent of DAC (assume A to be 94% of 100% DAC flaw signal after changing attenuator 25 dB).
3. Calculate the relative flaw signal amplitude (A_2) from the relation:

$$\text{change in dB} = 20 \log_{10}(A_2/A_1) ,$$

then

$$25 = 20 \log_{10}(A_2/94\%) \text{ and } A_2 = 1671\% .$$

Thus, for this example, the flaw signal equals 1650% of the maximum amplitude in percent DAC when rounded to the nearest 50%.

Length Measurements

The results of length measurements for the machined notches and EB weld cracks in block 4 appear in Table 3 for both 45 and 60° beams. The lengths were listed as the mean of each data set together with the standard deviation. The means were compared with the actual lengths, and the percentage errors are listed as an indication of the accuracy of the measurements. The standard deviations were also listed in the form of a percentage of the true length under the heading of random uncertainty. The ability to repeat the length measurements was excellent for all cases considered in specimen block 4. This fact was indicated by the low random uncertainty, with a maximum uncertainty of ±2.5% for a 45° beam angle and ±6.5% for a 60° beam. The random uncertainties listed for the flaw length measurements in block 4 were based on data sets with 20 independent measurements for each flaw. The random uncertainties for data sets of three readings, such as suggested by the code procedure, would be higher in most cases (i.e., in some instances we noted that it may double). Also, the ability to repeat length measurements depends on taking proper

Table 3. Measurement of flaw lengths in block 4 (machined notches and electron beam weld cracks)[a]

Flaw	Measured length[b]		Error (%)	Random uncertainty[c] (%)
	(mm)	(in.)		
	Measured with 45° beam angle			
1	92.1 ± 1.8	3.63 ± 0.07	23.4	±2.4
2	80.7 ± 1.5	3.18 ± 0.06	15.5	±2.2
3	98.1 ± 1.3	3.86 ± 0.05	28.8	±1.7
5	56.5 ± 0.8	2.23 ± 0.03	17.7	±1.7
6	89.5 ± 1.3	3.52 ± 0.05	17.5	±1.7
	Measured with 60° beam angle			
1	96.0 ± 4.8	3.78 ± 0.19	28.7	±6.4
2	79.5 ± 3.3	3.13 ± 0.13	13.8	±4.6
3	99.9 ± 2.5	3.93 ± 1.0	31.0	±3.3
5	50.5 ± 1.1	1.99 ± 0.04	5.2	±2.4
6	90.9 ± 4.5	3.57 ± 0.18	19.0	±5.9

[a]Each data set consisted of 20 independent measurements.

[b]All flaw lengths are overestimated (see Table 2).

[c]Standard deviation expressed as a percentage of actual length.

precautions during manual scanning to avoid twisting the orientation of the search unit. The amplitude of the signal may change by several decibels if the angular orientation of the search unit changes by as little as 1 to 5° (Appendix). This source of uncertainty places major limitations upon both accuracy and repeatability of all measurements performed by manual scanning. The overall accuracy of the length measurements in block 4 was no worse than 31%. Lengths were overestimated typically by 15 to 20%. Lateral beam spread is probably a major contributor to inaccuracies in the length measurement of large flaws. That topic will be treated in more detail in a later section of this report. The inaccuracies in the length measurements are in general slightly larger for a 60° beam than for a 45° beam. This effect could partially result from the greater lateral beam spread for a 60° beam than for a 45° beam because the metal path length is greater between the search unit and the flaw for a 60° beam.[3] The inaccuracies in length measurements are about the same for EB weld cracks (flaws 3 and 6) and machined notches. The result of that comparison gives some indication that the results obtained in this work are applicable to natural flaws because the characteristics of EB weld cracks closely approach those of natural flaws (ignoring compressive stress conditions).

The results of length measurements for the circular saw cuts in block 3 appear in Table 4 for 45° and 60° beam angles. The random uncertainty in the results obtained with a 45° beam angle was relatively low, ≤7.5%. In contrast, the random uncertainty for measurements obtained with a 60° beam was significantly higher, with values ranging up to ±36% for flaw 5. That rather large uncertainty in the case of flaw 5 resulted from the low amplitude of the signal. In the results obtained with a 60° beam, a correlation is apparent between the amplitude of the receiving signal (Table 1) and the random uncertainty in measuring the flaw lengths. The amplitude of the received signal was, of course, directly related to the angular orientation of the flaw. The overall accuracy of length measurements in block 3 was within 28% error for measurements obtained with a 45° beam and within 38% for measurements obtained with a 60° beam. Again, in most cases the inaccuracies were larger for results obtained with a 60° beam than the corresponding results obtained with a 45° beam. However, in contrast to the nonangled flaws in block 4, certain flaw orientations produced underestimates (see Table 4). Also, the accuracy of length measurements appears to correlate with angular orientation of the flaw. As previously indicated (Table 1), six of the flaws in block 3 were arranged in pairs that were oriented to make equal angles toward and away from the search unit. For example, the plane of flaw 5 was oriented 15° away from the search unit (the plane of the flaw made an angle of 15° with respect to the surface normal) and the plane of flaw 8 was oriented 15° toward the search unit. Measurement accuracy was compared for each of the corresponding pairs: flaws 5 and 8, 6 and 9, and 7 and 10. The results for most cases indicate that the measurement of flaw length is more accurate when the reflector is oriented away from the search unit (only if the amplitude remains high enough to measure by code method).

The conclusions based upon the results of this work indicate that for surface flaws within the range of sizes considered [40–76 mm (1.6–3.0 in.)], the lengths are measured by Code procedures to inaccuracies no greater than 28% for results obtained with a 45° beam and 38% with a

Table 4. Measurement of flaw lengths in block 3 (saw-cut notches at different angles)

Flaw	Measured length (mm)	Measured length (in.)	Error (%)	Random uncertainty[a] (%)
	Measured with 45° beam angle[b]			
4	51.7 ± 0.6	2.04 ± 0.03	27.2	±1.9
5	46.0 ± 0.4	1.81 ± 0.02	13.1	±1.25
8	52.1 ± 0.7	2.05 ± 0.03	28.2	±1.9
6	45.6 ± 0.5	1.76 ± 0.02	12.2	±1.1
9[c]	32.6 ± 3.3	1.28 ± 0.13	−19.9	±7.5
7	48.9 ± 1.9	1.93 ± 0.08	20.3	±5
10	46.7 ± 0.8	1.84 ± 0.03	14.9	±1.9
	Measured with 60° beam angle[d]			
4	46.7 ± 2.0	1.84 ± 0.08	14.9	±4.8
5[e]	38.9 ± 14.5	1.53 ± 0.57	−4.2	±35.8
8	55.2 ± 6.0	2.17 ± 0.24	35.8	±14.8
6	48.9 ± 1.4	1.92 ± 0.05	20.2	±3.3
9	56.3 ± 1.4	2.22 ± 0.10	37.5	±6.3
7	*f*	*f*	*f*	*f*
10	49.6 ± 4.4	1.95 ± 0.17	22.0	±10.8

[a]Standard deviation expressed as a percentage of actual length.

[b]Each data set consisted of 10 independent measurements.

[c]The only notch underestimated in length (surface lengths about 41 mm) (angled 30° toward search unit).

[d]Each data set consisted of 20 independent measurements.

[e]The only notch underestimated in length (surface lengths about 41 mm) (oriented 15° away from search unit).

[f]Not measurable with 60° beam (oriented 45° away from search unit).

60° beam. Additionally, the lengths are generally overestimated except for certain angular orientations that provide underestimates. These conclusions apply only to the case of a 25.4-mm (1.00-in.) circular transducer with a frequency of 2.25 MHz and manual scanning.

Correlation Between the Magnitude of Lateral Beam Spread and Flaw Length Measurements

The lateral beam spread from the transducer has a known influence on the measurement of flaw lengths. However, no code-recommended method is available for the measurement of lateral beam spreads. A technique developed at ORNL has allowed the measurement of lateral beam spreads in thick pressure vessel steel.[3] Use of that development established a relationship that permitted the determination of the lateral beam spread (increase in beam width normal to the beam axis) for any path length in the metal.

Of particular interest were the noted characteristics of instrument I (with the tuning switch set in the 0.5- to 2.5-MHz position) with a bandwidth at −20 dB of from 0.2 to 5.5 MHz and a center frequency of 0.9 MHz.[4] When, however, the tuning switch of instrument I was placed in the 2- to 8-MHz position (either position is valid for the 2.25-MHz search unit), the bandwidth at −20 dB extended from 1.9 to 11 MHz with a center frequency of 5.5 MHz.[4] The resulting beam spreads corresponding to the two different tuning positions are shown in Fig. 11. Also shown in Fig. 11 is the resulting beam spread for instrument II. Referring to

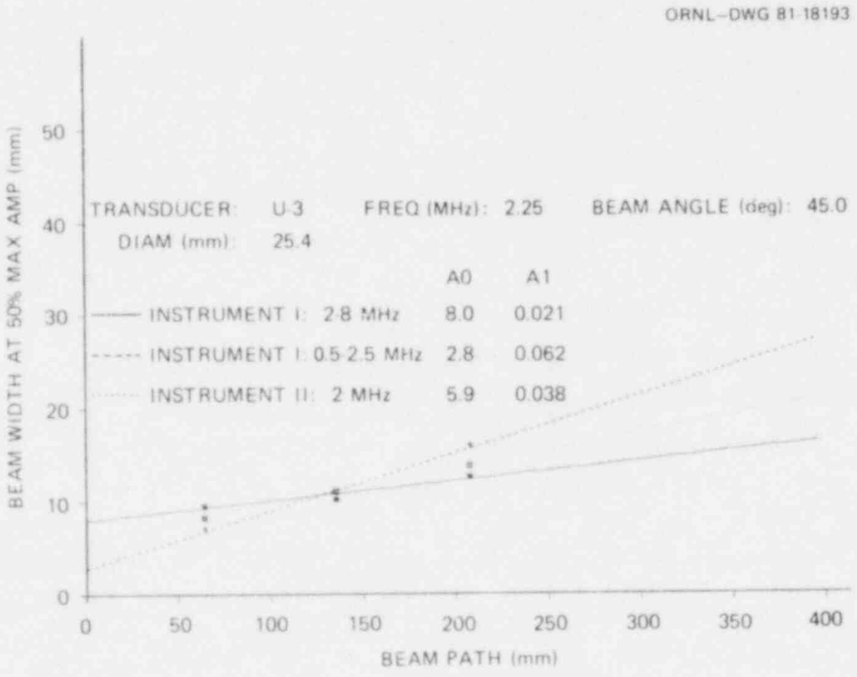

Fig. 11. Lateral beam spread curves obtained with commercial instrument I (two tuning positions) and commercial instrument II. Data are fit by lines BAND WIDTH = A0 + A1(BEAM PATH).

Fig. 11, the lateral beam width is determined from the appropriate curve and beam path length in each case.[3] As can be seen from this figure, the ultrasonic signal that had the higher center frequency has the smaller of measured beam spreads (as expected theoretically).

To correlate the magnitude of lateral beam spread with the measurement of flaw length, a number of measurements were made with the two receiver tuning positions on instrument I and all other variables held constant. The results of the flaw length measurements in block 4 are indicated in Table 5. In each case the measured flaw length was clearly greater when measured in the tuning position with the larger beam spread (lower center frequency). This difference was substantially greater than the random uncertainties represented by the standard deviation in each case. Therefore it is evident that lateral beam spread contributes a substantial systematic error in the measurement of flaw lengths. This effect was not quite as great for flaw 3, which corresponded to an EB weld crack; however, the correlation was clearly demonstrated.

Table 5. Correlation between magnitude of lateral beam spread and measurements of flaw length in block 4 (search unit U-3 and instrument I)

Flaw[a]	Measured length, mm (in.)	
	Smaller beam spread[b]	Larger beam spread[b]
1	95.18 ± 0.8 (3.77 ± 0.03)	99.5 ± 0.8 (3.92 ± 0.03)
2	85.7 ± 0.0 (3.38 ± 0.0)	89.0 ± 0.8 (3.51 ± 0.03)
3	99.06 ± 0.9 (3.91 ± 0.04)	101.4 ± 0.8 (3.99 ± 0.03)

[a]Refer to Table 2 for a description of the flaws in block 4.

[b]Refer to Fig. 11 for a graphical representation of the two beam spreads.

Beam Spread Corrections for Length Measurements

Since the lateral beam spread from the transducer has an obvious influence on the measurement of flaw lengths, we tried to apply a correction to the measurement of flaw lengths. Using the relationship discussed in the previous section for instrument II (Fig. 11), we established the beam width for the flaws located in both blocks 3 and 4. The correction applied in each case was to subtract the appropriate beam width from the length measurement (50% of DAC). The results of the beam spread corrections to the flaw lengths for a beam angle of 45° appear in Table 6. The results for the nonangled flaws (block 4) are more accurate than those for the flaws that contain the flaw orientation variables (block 3). For example, the longer deeper flaw (notch 1) in block 4 was very accurately measured with the beam width correction (+2.5%). For notch 2 (block 4),

Table 6. Beam width corrections to flaw length measured with a 45° beam angle

Flaw	Without beam width corrections			With beam width corrections[a]		
	Length		Error (%)[b]	Length		Error (%)[b]
	(mm)	(in.)		(mm)	(in.)	
	Block 4 (machined notches and electron beam weld cracks)					
1	92.1 ± 1.8	3.63 ± 0.07	+23.4	76.6	3.02	+2.5
2	80.7 ± 1.5	3.18 ± 0.06	+15.5	65.2	2.57	–6.7
3	98.1 ± 1.3	3.86 ± 0.05	+28.8	82.6	3.25	+8.4
5	56.5 ± 0.8	2.23 ± 0.03	+17.7	41.0	1.61	–14.6
6	89.5 ± 1.3	3.52 ± 0.05	+17.5	74.0	2.91	–2.9
	Block 3 (saw-cut notches at different angles)					
4	51.7 ± 0.6	2.04 ± 0.03	+27.2	35.6	1.63	–13.2
5	46.0 ± 0.4	1.81 ± 0.02	+13.1	29.9	1.40	–27
8	52.1 ± 0.7	2.05 ± 0.03	+28.2	36.0	1.65	–12.2
6	45.6 ± 0.5	1.76 ± 0.02	+12.2	29.5	1.39	–28
9	32.6 ± 3.3	1.28 ± 0.13	–19.9	16.5	0.88	–59.8
7	48.9 ± 1.9	1.93 ± 0.08	+20.3	32.8	1.52	–20
10	46.7 ± 0.8	1.84 ± 0.03	+14.9	30.6	1.44	–25.4

[a]The correction (15.5 mm for block 4, 16.1 mm for block 3) was taken from Fig. 11 (instrument II).

[b]Based on the actual lengths shown in Table 2 for block 4, 41 mm for block 3. + indicates overestimate, –, underestimate.

which is shallower, a substantial improvement in accuracy is still evident. Notches 3 and 6, which are EB weld cracks, again are measured more correctly in length with beam width correction, even though the natural-like flaws should have more variability in ultrasonic response than machined flaws. The result for notch 5 provides the largest deviation (block 4) probably (1) because it is relatively shallower (same depth as notch 2), and (2) because of its shape. Notch 5 is a circular saw cut with a 50.8-mm (2.00-in.) radius and 5.6-mm (0.25-in.) depth. Thus, the flaw depth is essentially zero (as far as being a reflector of 2.25-MHz ultrasound) at each of the feathered ends. Thus, the effective amplitude of the signal is being affected by both the decreasing depth of the flaw and the movement of the sound beam off the end of the flaw. Yet the error of –14.6% (Table 6) relates to the surface length of the

elliptical reflectors. Also, note that notch 4 in block 3 (Table 6) has a length error of −13.2% after correcting for beam width. This notch is very similar to notch 5 in block 4 (saw cuts of 4.6 and 5.6 mm depths respectively). Both are very good simulators of the flaws addressed by Sect. XI, Paragraph IWB-3500, of the ASME code, where aspect ratios are used to determine the acceptability of surface-oriented or buried flaws (the flaws are smaller at the ends). This is also true of the angled saw cuts in block 3, for which beam width corrections may have to be decreased (because of flaw shape) to account for decreasing flaw response at the ends (especially if orientation introduces another variable). From Table 6, all saw-cut notch lengths except for notch 9 would be significantly improved if a bias were introduced into the beam width correction to account for flaw shape (i.e., about half the lateral beam width should be subtracted from the measured length). Thus, a more conservative approach to correcting the overestimated flaw length [which appears to account for elliptical (saw-cut) surface-connected flaws] would be to reduce the measured length by one-half the lateral beam width measured at the appropriate depths.

Depth Measurements

The depth measurements reported in this section were collected by the manual flaw measurement technique described by the code (Sect. V, Article IV, Appendix D-10) as supplemented by the method developed for FSH signals (see the section in this report on procedures used for depth measurement). Thus, any discussion of code depth measurement assumes that the FSH supplement is a code-acceptable version of Appendix D-10.

The results of the measurement of flaw depth for the machined notches and EB weld cracks of block 4 appear in Table 7 for beam angles of both 45 and 60°. As in the case of length measurements, the depths were stated in the form of a mean for each data set along with the standard deviation. The standard deviations were expressed as a percentage of actual depths and listed under the heading of random uncertainty. As before, the random uncertainty is an indication of the ability to repeat the measurement. The random uncertainties for block 4 were up to 28% for a beam angle of 45° and up to 36% for 60°. The repeatability of depth measurements was in every case better for measurements made with a 45° beam angle than those made with 60° beam angle. There were no apparent differences between the random uncertainties for the EB weld cracks (flaws 3 and 6) and the machined notches. The accuracy of the depth measurements was, as in the case of length measurements, expressed by a percent error comparison between the mean of each data set and actual flaw depths. Measurements made with both 60 and 45° beams had a much greater percent error for the smaller machined flaws 2 and 5 than for the deeper machined notch 1. This fact indicated a dependence of measurement accuracy on actual flaw depth. The actual depths of both flaws 2 and 5 were 6.4 and 5.6 mm (0.25 and 0.22 in.). In comparison, the depths of the EB weld cracks (flaws 3 and 6) were 9.5 mm (0.38 in.), and the errors involved in the measurement of those depths were again significantly smaller. Overall, the depths are generally overestimated for shallower flaws. There seemed to be no significant differences between depth measurements of EB weld cracks and machined notches. In fact, with this code procedure, a trend

Table 7. Measurement of flaw depths in block 4 (machined notches and electron beam weld cracks)[a]

Flaw	Measured depth (mm)	Measured depth (in.)	Error (%)[b]	Random uncertainty (%)[c]	Real depth (mm)	Real depth (in.)
		Measured with 45° beam angle				
1	11.5 ± 0.7	0.45 ± 0.03	−10	±6	12.7	0.50
2	11.2 ± 1.7	0.44 ± 0.07	+76	±28	6.4	0.25
3	11.5 ± 1.5	0.45 ± 0.06	+20	±16	9.5	0.38
5	10.7 ± 1.4	0.42 ± 0.06	+91	±24	5.6	0.22
6	9.2 ± 1.9	0.36 ± 0.08	−4	±21.3	9.5	0.38
Average	10.8 ± 1.0	0.42 ± 0.04				
		Measured with 60° beam angle				
1	15.6 ± 1.5	0.61 ± 0.06	+22	±12	12.7	0.50
2	14.5 ± 1.3	0.57 ± 0.05	+128	±20	6.4	0.25
3	12.1 ± 1.8	0.47 ± 0.07	+25.3	±18.7	9.5	0.38
5	11.2 ± 2.4	0.44 ± 0.09	+100	±36	5.6	0.22
6	12.7 ± 1.7	0.50 ± 0.07	+33.3	±18.7	9.5	0.38
Average	12.9 ± 1.6	0.51 ± 0.06				

[a]Each data set consisted of 10 independent measurements.

[b]Percent measurement over (+) or under (−) actual maximum flaw depth.

[c]Standard deviation expressed as a percentage of actual depth.

is to measure a nominal depth regardless of the real depth of the notches. For example, if the statistical average of the depth measurements made at 45 and 60° (Table 7) is calculated, the average calculated (measured) depths are 10.8 mm (plus or minus a standard deviation of 1.0 mm) and 12.9 mm (plus or minus a standard deviation of 1.6 mm) respectively. Although, in this study, only limited depths were available (5.6, 6.4, 9.5, and 12.7 mm as shown in Table 7), the flaw depths cover a range significant to the code.

The results of depth measurements for the circular saw cuts in block 3 appear in Table 8. Both repeatability and accuracy were very poor for depth determination in specimen block 3 and in all cases depths were grossly overestimated for both beam angles. Again, a trend is noted in the depth measurement data to read a nominal depth regardless of the notches' real depths. For example, the average depth measurement with a 45° beam angle is 10.5 mm (plus or minus a standard deviation of 1.4 mm) and with a 60° beam angle is 13.3 mm (plus or minus standard deviation of 1.3 mm).

Table 8. Measurement of flaw depths in block 3 (saw-cut notches at different angles)[a]

Flaw	Measured depth (mm)	Measured depth (in.)	Error[b] (%)	Random uncertainty (%)[c]
	Measured with 45° beam angle			
4	12.3 ± 2.7	0.49 ± 0.11	+272	±61.1
5	8.7 ± 1.8	0.34 ± 0.07	+96.5	±40.5
8	10.1 ± 0.1	0.40 ± 0.04	+131	±23
6	10.7 ± 1.6	0.42 ± 0.06	+171	±38.7
9	10.5 ± 2.2	0.42 ± 0.08	+170.9	±51.6
7	9.0 ± 1.3	0.36 ± 0.05	+183	±39.4
10	12.1 ± 2.0	0.47 ± 0.08	+270	±63
Average	10.5 ± 1.4	0.41 ± 0.06		
	Measured with 60° beam angle			
4	11.8 ± 1.9	0.46 ± 0.07	+156	±38.9
5	11.5 ± 2.5	0.45 ± 0.10	+160	±57.8
8	14.5 ± 1.9	0.57 ± 0.07	+230	±40.5
6	14.5 ± 1.9	0.57 ± 0.07	+268	±45.0
9	14.0 ± 2.0	0.55 ± 0.08	+255	±51.6
7	*d*	*d*	*d*	*d*
10	13.7 ± 1.8	0.54 ± 0.07	+212	±55.1
Average	13.3 ± 1.3	0.52 ± 0.05		

[a]Each data set consisted of 10 independent measurements.

[b]Percent measurement over (+) or under (–) actual maximum flaw depth.

[c]Standard deviation expressed as a percentage of actual depth.

[d]Not measurable with 60° beam.

These measurements are almost identical to those reported for Table 7 even though the through-wall notch depth in all cases is less (all were cut about 4.6 mm with various angles to produce through-wall depths of 3.2, 4.0, 4.4, and 4.6 mm). As a further check on this observation, we made similar measurements on the end of the block (simulation of a through-wall flaw). This was done to see if the apparent size would be near the same value with the moving search unit measurement for planar flaws. We assumed that nearly identical measurements from the end of the block may indicate that both the flaws' reflectivity characteristics (corner effect) and the relative search unit (detector) position are major factors in the depth measurement. A simple measurement from block 4, where a smooth machined right-angle corner was available, indeed measured it at about 9 mm (with a 45° beam). When, however, an unmachined rough near-right-angle corner of block 4 was measured by the same FSH-supplemented code techniques (45° beam), values up to 17 mm were measured. The largest depth (17 mm) was not as reproducible as the one for the higher amplitude machined corner (because it was more difficult to reproduce the signal from the rounded or rough corner). However, it was evident and expected that the measured depth by the code method is affected by the reflector orientation, shape, and roughness. It also appears that the absolute amplitude of the signal may be affecting the depth measurement (e.g., the 8 dB lower amplitude nonmachined corner measured about double the machined corner reflector). Also Table 2 indicates that the amplitude increases for increasing flaw depth; however, these reported amplitudes represent one or two measurements and not a statistical average for multiple measurements.

We also noted that the end of the block signal measured from 2000 to 3000% of DAC. Thus, more accurate planar flaw depth measurements may be possible if the moving search unit measurement accounted for maximum amplitude and beam width effects. It is not yet readily apparent how this might be done. In any event, our limited data clearly show that for smaller flaw depths (e.g., 4.6 mm or smaller), errors as much as 272% are measured with the Code method (see Table 8, notch 4). It is also obvious that very large flaws may be underestimated (e.g., the end of the block). The smallest error is noted for 9 to 13 mm depths with the 45° beam (see Table 7, notches 1, 3, and 6).

As previously stated, these conclusions apply only to the conditions actually tested in this confirmatory work: 2.25-MHz, 25.4-mm-diam (1.00-in.) circular transducer with beam angles of 45 and 60°, manual scanning, and simulated flaws on the surface. Also, for any size surface-breaking flaw, we feel that the corner effect will place additional limitations upon the ability to accurately determine the depth according to current code techniques.

BURIED FLAWS

The interpretation of results of depth measurements on the buried flaw was somewhat complicated because a portion of side-drilled hole protruded into the flat plane of the vertical saw cuts (Fig. 7). (Thus, it was more easily detected than a true planar midplane flaw would have been.) However, we could distinguish the portion of the signal emanating

from the side-drilled hole. The only signals detectable from the flat portion of the midplane flaw were those resulting from diffraction from each edge (detectable at code calibration level at 45° but not at 60°). Using the two signals from the upper and lower edges, we could measure the depth of the flaw with a 45° beam. The results of that measurement indicated a depth of 29.2 ± 1.7 mm (1.15 ± 0.07 in.) with a possible 30% error. The attempt to measure the depth with a 60° beam was not successful. Only the signal from the upper edge was detected, and it was well below 50% DAC. Even though a measurement of depth was made with a 45° beam, it would be difficult for an operator to interpret the two edge signals obtained with a single-transducer technique without prior knowledge of the geometry of the flaw. Furthermore, the signals diffracted from the edge of a natural flaw would in all probability be much lower in amplitude (i.e., lower than the 50% DAC limits set by the code). The conclusion, based upon the results of this confirmatory work, indicate that the single-transducer technique is not suitable for detecting or measuring a midplane flaw oriented perpendicular to the surface of the vessel. Either a two-probe tandem technique or a multiple-transducer array would be suitable for detecting flaws of that nature. The use of such techniques is well documented.[5]

CONCLUSIONS AND RECOMMENDATIONS

Flaw detection capabilities for the limited numbers of surface-breaking simulated flaws used in this study (Tables 1 and 2 document the simulated flaws and the ultrasonic amplitude response) appear to be quite good, with the exception of flaw 7 in block 3 (see Table 1). Flaw 7 would have been detected also if the search had been performed in both directions (evident from the 60° response on flaw 10 in Table 1). Thus, no changes to the code are recommended for the detection of flaws located on the opposite surface from the search unit (i.e., those that provide a corner trap condition).

Measurement of flaw length with code techniques (again based on limited, but substantial, simulated surface flaws) always overestimated the actual length. In fact, except for saw-cut notches, the 45° angle beam overestimated the length by an amount very near the beam width at the flaw depth. Thus the first recommendation would be to correct flaw length by this amount. However, since elliptical flaws similar in effective reflecting area to saw cuts are a basic rejection shape (Sect. XI, Paragraph IWB-3500, of the ASME Code), and since these types of reflectors were overestimated by about half the beam width at the proper flaw depth (especially if measured from both directions and the larger measured length selected), a change in the code is recommended that would reduce the measured flaw length (for a surface-breaking flaw opposite the search surface) by one-half the lateral beam width at the appropriate flaw depth.

Measurement of flaw depths with code techniques (again based on limited, but substantial, simulated surface flaws) indicated a trend to measure a nominal depth regardless of the real depth. In any event, significant errors obviously occur in the flaw depth measurements by the existing code techniques and accurate depth measurements appear to be

limited to a specific narrow depth range (i.e., very shallow flaws are overestimated and very deep flaws are underestimated). Thus, we recommend that the code method for measuring flaw depth be altered and/or supplemented by alternative techniques that are established by developmental studies encompassing more flaws than were considered in this report. Improvements in measuring flaw depth (based on the basic code approach of amplitude of signal and transducer movement) may be possible through the use of different size or multiple transducers. Focused search unit techniques could improve depth measurements (or at least extend the measurement range) because they should not be as prone to search unit movement limitations (i.e., less surface scan may be required to make measurements on somewhat deeper flaw measurements).

A non-surface-breaking, or buried, flaw was used for a very limited study; however, results did show that both detection and measurement can be problems with the current code techniques. Thus, it is fairly obvious that alternative techniques are necessary to detect and measure flaws located near midplanes and oriented perpendicular to the vessel surface, and we recommend that supplementary scanning be employed (e.g., two-search-unit tandem techniques or multiple transducer arrays).

ACKNOWLEDGMENTS

The authors would like to thank J. C. Lewis for helping with the data collection, the collection of beam spread data, and many useful suggestions. We also thank Serge Boudreault for contributing to the collection of data, J. H. Smith and G. W. Scott for technical contributions, J. L. Bishop for preparation of the manuscript, S. Peterson for editing, and S. G. Frykman for preparation of the final report.

REFERENCES

1. J. G. Merkle et al., "Flaw Preparation," *Test of 6-in.-Thick Pressure Vessels. Series 3: Intermediate Test Vessel V-7*, ORNL/NUREG-1, September 1976, pp. 19–22.

2. T. D. Jamison and W. R. McDearman, *Studies on Section XI Ultrasonic Repeatability*, EPRI-NP-1858, Electric Power Research Institute, Palo Alto, Calif., May 1981.

3. K. V. Cook, P. J. Latimer, R. W. McClung, and K. K. Klindt, *Ultrasonic Beam Spread Measurements in Thick Pressure Vessel Type Steel*, NUREG/CR-2485, ORNL/TM-8159, February 1982.

4. J. Krautkrämer, Manual Issue 9,23731-2,930, Ultrasonic Flaw Detector USIP11, Krautkrämer-Branson International, Cologne.

5. J. Krautkrämer and H. Krautkrämer, "Welded Joints," Chap. 26, pp. 466–564, and "Nuclear Reactors," Chap. 28, pp. 518–25 in *Ultrasonic Testing of Materials*, 2nd ed., Springer-Verlag, New York, 1977.

Appendix

THE INFLUENCE OF THE ANGULAR ORIENTATION OF THE SEARCH UNIT UPON THE RECEIVED AMPLITUDE FROM THE FLAW

The angular orientation of the search unit (relative to the normal of a planar flaw) has a significant influence on the amplitude of the received signal from a flaw. Consequently, the measured dimensions of a flaw (by use of an amplitude-based technique) also depend greatly on the angular orientation (skew) of the search unit and on any changes in angular orientation during scanning. The purpose of the work presented in this appendix is to establish a quantitative relationship between angular orientation of the search unit and the received amplitude from a flaw.

The data were taken with a mechanical scanner (Fig. A.1). The scanner provided a great deal of stability, precision motion, and angular positioning with a readout to 0.02°. The essential component of the scanning device was a lathe bed with special devices on the tool post for attaching fixtures for the search units. The scanning was done in conjunction with a water box to provide the couplant. The transducer used for the collection of data was a round, 2.25-MHz, untuned, commercially manufactured transducer with ORNL serial number U-1. This transducer was almost

ORNL-PHOTO 0872-78

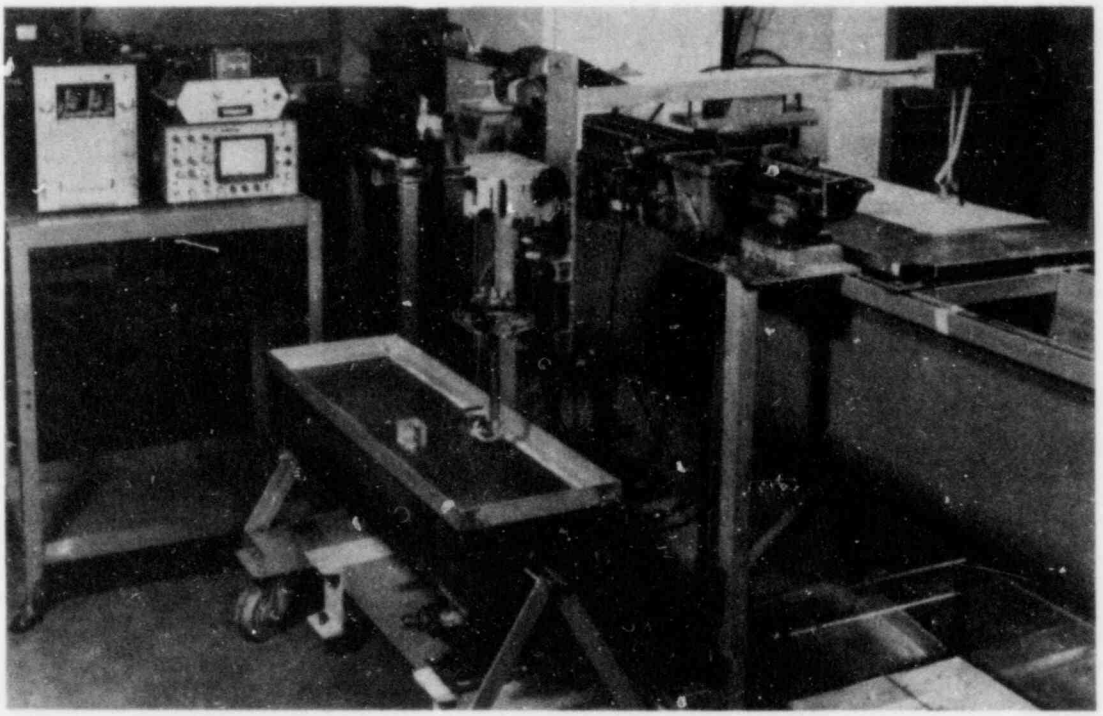

Fig. A.1. Mechanical scanner.

identical with the transducer used for the collection of data in the previous sections of this report. The instrument used for the collection of data was commercial instrument II tuned to the 2-MHz position.

Beam angles of 45 and 60° were used in this study. In each case the flaw was a planar flaw or a planar crack [electron beam (EB) weld crack] normal to the surface of the specimen block. The two specimen blocks used were block 4 (Fig. 10) and block 2. The surface flaws introduced into block 2 were identical in every respect with those in block 4. Therefore, Fig. 10 describes the flaw geometry in both blocks 4 and 2.

The angular orientation of the search unit was adjusted about an axis normal to the surface of the specimen block, as shown in Fig. A.2. The initial amplitude was maximized (to the same approximate magnitude in each case), and then successive scans parallel to the notch were made with angular orientation increments of either 1 or 2° (referenced perpendicular to the notch). For each successive scan the received amplitude was recorded on a strip chart along with an index mark for designating the angular setting for that particular scan.

Typical results from block 2 are presented in Figs. A.3 and A.4. Some immediate conclusions can be drawn from the data presented in the figures. First, from the shape of the amplitude response, the general nature of the flaw was immediately apparent. The jagged signal was characteristic of an EB weld crack. The relatively smooth-amplitude signal was, on the other hand, characteristic of a machined notch.

For the particular transducer used in this study, the received amplitude from the flaw was down to noise level when the angular orientation of the search unit had reached from 8 to 9° on either side from the maximum amplitude (0°) position. The angular change necessary to reduce the signal amplitude to noise level was in general the same for both beam angles of 45 and 60° as well as for both machined notches and EB weld cracks.

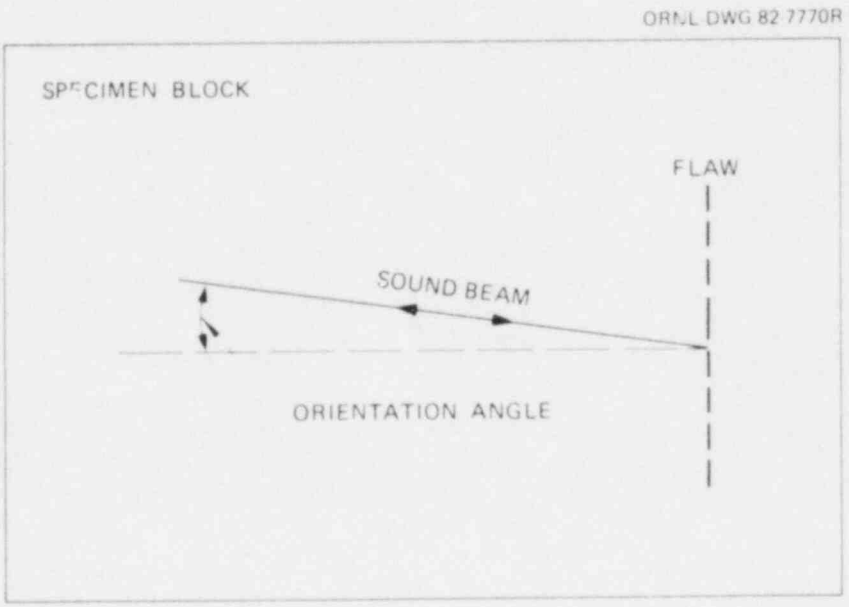

Fig. A.2. Plan view of scanning setup showing angular orientation.

ORNL-DWG 81-20586R

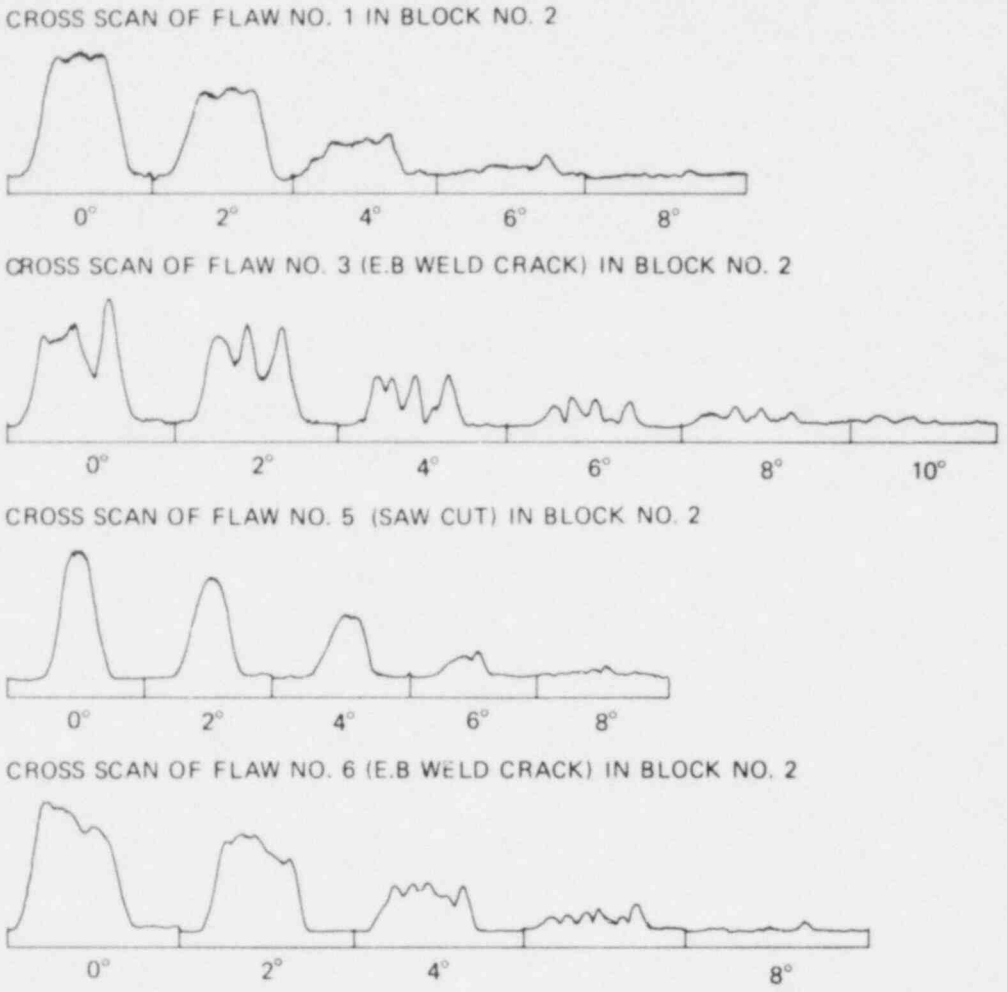

Fig. A.3. Received amplitude as a function of angular orientation of the search unit (45° beam angle). Block 2 is a duplicate of block 4 (see Table 2 and Fig. 10 for description of simulated flaws).

ORNL-DWG 81-20587

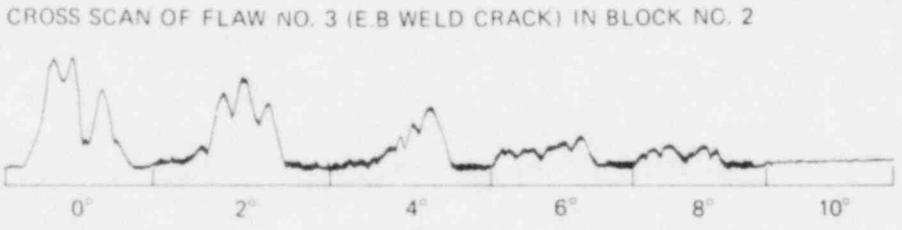

Fig. A.4. Received amplitude as a function of angular orientation of the search unit (60° beam angle). Block 2 is a duplicate of block 4 (see Table 2 and Fig. 10 for description of simulated flaws).

The decrease in amplitude per degree of change in angular orientation, in general, increased as the total angular change increased from the position of peak amplitude response. For this test system the average drop in amplitude was 3.8 dB/deg for the 45° beam angle and 1.9 dB/deg for the 60° beam angle.

The amplitude response was reasonably symmetrical with respect to changes in angular orientation in both directions. Thus, only one direction is shown in Figs. A.3 and A.4. The symmetry was generally greater for the machined notches than for the EB weld cracks.

The impact of this study upon flaw measurement is clearly evident. In manual scanning, a change in angular orientation of from 1 to 2° could change the amplitude of the received signal by as much as 8 dB. This variable change in amplitude over a scan constitutes a highly significant source of error in the measurement of a flaw by code techniques. This places a major limitation upon the reliability of measurement by manual scanning unless some provision (e.g., mechanical fixturing) is made to keep the angular orientation constant throughout the scan.

NUREG/CR-2661
ORNL/TM-8295
Distribution
Category R5

INTERNAL DISTRIBUTION

1–2. Central Research Library
3. Document Reference Section
4–5. Laboratory Records Department
6. Laboratory Records, ORNL RC
7. ORNL Patent Section
8. R. G. Berggren
9. R. S. Booth
10. R. A. Bradley
11. R. H. Bryan
12. R. O. Cheverton
13–17. K. V. Cook
18. W. Fulkerson
19–21. M. R. Hill
22. F. J. Homan
23. R. C. Hudson
24. E. B. Johnson
25. K. K. Klindt
26. A. L. Lotts
27. F. C. Maienschein
28–32. R. W. McClung
33. J. G. Merkle
34. G. N. Miller
35. R. K. Nanstad
36. L. B. Shappert
37. G. M. Slaughter
38. J. H. Smith
39. C. R. Weisbin
40. G. D. Whitman
41. L. C. Williams

EXTERNAL DISTRIBUTION

42. NRC, OFFICE OF NUCLEAR REGULATORY RESEARCH, Washington, DC 20555
Program Sponsor

43. DOE, OAK RIDGE OPERATIONS, OFFICE, P.O. Box E, Oak Ridge, TN 37830
Office of Assistant Manager for Energy Research and Development

44–45. DOE, TECHNICAL INFORMATION CENTER, P.O. Box 62, Oak Ridge, TN 37830

46–430. For Distribution Category R5 (10 — NTIS)

☆ U.S. GOVERNMENT PRINTING OFFICE